Master's Thesis

석사 학위논문

A Study on Dual SMART System

for Bimanual Microsurgery

Hyun-cheol Park（박 현 철 朴 賢 哲）

Department of Robotics Engineering

로봇공학전공

DGIST

2016

Master's Thesis

석사 학위논문

A Study on Dual SMART System

for Bimanual Microsurgery

Hyun-cheol Park（박 현 철 朴 賢 哲）

Department of Robotics Engineering

로봇공학전공

DGIST

2016

A Study on Dual SMART System

for Bimanual Microsurgery

Advisor	:	Professor Cheol Song
Co-advisor	:	Professor Jae youn Hwang

By

Hyun-cheol Park
Department of Robotics Engineering
DGIST

A thesis submitted to the faculty of DGIST in partial fulfillment of the requirements for the degree of Master of Science in the Department of Robotics Engineering. The study was conducted in accordance with Code of Research Ethics[1]

01. 08. 2016

Approved by

Professor   Cheol Song   (Signature)
                    (Advisor)

Professor   Jae youn Hwang   (Signature)
                    (Co-Advisor)

---

[1] Declaration of Ethical Conduct in Research: I, as a graduate student of DGIST, hereby declare that I have not committed any acts that may damage the credibility of my research. These include, but are not limited to: falsification, thesis written by someone else, distortion of research findings or plagiarism. I affirm that my thesis contains honest conclusions based on my own careful research under the guidance of my thesis advisor.

A Study on Dual SMART System

for Bimanual Microsurgery

Hyun-cheol Park

Accepted in partial fulfillment of the requirements
for the degree of Master of Science.

11. 24. 2015

Head of Committee	Prof. Cheol Song	(인)
Committee Member	Prof. Jae youn Hwang	(인)
Committee Member	Prof. Jaesung Hong	(인)

ABSTRACT

Manual micro-surgical tasks are fundamentally divided into grasping, cutting and injecting maneuvers performed on biological tissues. Efficient dissection of fibrous tissue from the retina often requires grasping and cutting maneuvers which are carried out simultaneously. True bimanual surgery requires that the surgeon overcomes the hand tremor of both hands at once as well as unpredicted patient's movement.

In this study, we develop and evaluate a dual SMART micro-surgical system for bimanual surgery. The dual SMART system is composed of two common-path swept source optical coherence tomography (CP SS-OCT) distance sensor with a ball lens, two piezoelectric (PZT) motor and customized horizontal scissors and forceps. The ball lens coupled OCT distance sensor could detect the unintended tremor in both hands at tilted angle from 90 to 45 degree. Also, high numerical aperture (NA) of the ball lens coupled OCT sensor has 1.3 times higher signal-to-noise-ratio (SNR) than bare fiber based OCT sensor.

In order to achieve efficient bimanual dissection, each end-effector's desired height could be controlled by the dual SMART system. Total feedback control rate of the system is nearly 500 Hz which is enough to compensate the hand tremor of 6-12 Hz. Additionally, customized horizontal scissors and forceps contribute to accessibility of surgical area compared to commercial vertical scissors and forceps.

Results of hand tremor cancellation demonstrate that the ball lens coupled dual SMART system could compensate unpredictable tremor in various tilt angles even in water. The dual SMART system could precisely dissect an egg membrane compared to freehand. The root mean square error (RMSE) of dual SMART is about 10 times smaller than freehand one. Furthermore, dissected surface of the membrane by the system was uniformed. The system with high SNR proved that it could compensate the tremor in a porcine eye compared to freehand.

The improved dual SMART system will be useful for bimanual vitrectomy with minimized iatrogenic damage. In the future, durability of the dual SMART system should be improved for the stable microsurgery.

Contents

List of Figures

1. INTRODUCTION

1.1 Objectives and Motivations

Microsurgery requires safe and accurate manipulation of the surgical tools due to the limitations of small surgical spaces. Specialized micro-surgical tasks are limited by physiological conditions and difficulty of flexible motion of micro-surgical tools. Most microsurgeries could be implemented with microscope and micro-surgical instruments. For example, it is difficult to delete scar tissues delicately in retinal detachment of vitrectomy. It is hard to percept depth information with respect to optical axis using a microscope. Various imaging systems to provide the depth information with surgeons have been followed [1-4] Also, physiological hand tremor prevent micro-surgeons from completing the assigned tasks without any surgical errors. The hand tremor has 0-15 Hz frequency on the order of 100 um of unpredictable motion magnitude [5]. There has been various approaches to compensate the one hand's tremor as followed: Micron [6-9], micro-surgical system using Steady-hand robot [10-20], SMART [21-27], other handheld device for microsurgery [28-38]. They have mainly focused on stabilizing an end-effector of the surgical tool. These systems assisted one-handed micro-manipulation could not assist to fix, dissect, and aspirate the surgical target precisely and safely because most of the internal scar tissues are made up of soft, limp, and aqueous materials.

However, bimanual microsurgery could allow grasping and precise dissection simultaneously regardless of the characteristic of the biological tissue [39,40]. Some bimanual micro-surgical systems and methods have been proposed [40-42]. The bimanual haptic forceps system could precise manipulation by two delta robot. Because this system are heavy, the surgeons may be felt uncomfortable. The fiber optic-free micro-surgical

system could operate without internal light pipe. The system could not suppress the tremor of both hands.

In this paper, we present a bimanual micro-surgical system using the ball-lens coupled common-path swept source optical coherence tomography (CP SS-OCT) distance sensors and two piezoelectric (PZT) motors. Asynchronous tremor of both hands could be compensated by the PZT motors while the CP SS-OCT distance sensor could detect height variation of each end-effector. Micro-surgeons could simultaneously grasp and dissect a surgical target on the desired height. In the dissection of the biological tissues, the proposed bimanual SMART system has enhanced surgical performance, compared to freehand.

1.2 Background and information

1.2.1 History of microsurgery

The word 'Microsurgery' is for surgery requiring an operating microscope. The blood vessels and nerves (less than 1 mm) which could transfer from one lesion of the body to another by re-attaching of severed parts. Over the past years, the otolaryingologists started microsurgical techniques. A Swedish otolaryngologist, Carl-Olof Siggesson Nylén (1892–1978), was the father of microsurgery. In 1921, in the University of Stockholm, he built the first surgical microscope, a modified monocular Brinell-Leitz microscope. At first he used it for operations in animals. In November of the same year he used it to operate on a patient with chronic otitis who had a labyrinthine fistula. Nylen's microscope was soon replaced by a binocular microscope, developed in 1922 by his colleague Gunnar Holmgren (1875–1954).

The operating microscope initiated to be used for ear surgery. In the 1950s many otologists began to use it in the fenestration procedure, usually to perfect the opening of the fenestra in the lateral semicircular canal. The revival of the stapes mobilization operation by Rosen, in 1953, made the use of the microscope mandatory, although it was not used by the originators of the technique, Kessel (1878), Boucheron (1888) and Miot (1890). Mastoidectomies started to be performed with the surgical microscope and so were the tympanoplasty techniques that became known in the early 1950s. [43]

Now, microsurgery is being utilized by various surgical field such as 'opthalmology,' 'neurosurgery,' 'otolarynggology,' 'orthopedic surgery,' and 'plastic surgery' and so on.

1.2.2 Bimanual vitrectomy

Bimanual vitrectomy requires two surgical instrument to manipulate retina tissue inside eye simultaneously. Especially, bimanual vitrectomy is applied to treat difficult cases of diabetic tractional retinal detachment (TRD) for the complete and safe elimination of epiretinal membranes (ERMs) [44]. The bimanual scheme is easy to grasp the membrane using forceps and separate membranes between retinal-surface by means of dissection by dissection using scissors.

Here, we focus on the compensation of bimanual hand tremor because untended bimanual hand tremors may damage to an eye during specific surgery and provide micro-surgeons with distance information between end-effector of surgical tools and target surface.

2. PRINCIPLE OF OPTICAL COHRENCE TOMOGRAPHY (OCT)

2.1 Chapter Overview

Optical coherence tomography (OCT) is one of cross-sectional imaging techniques such as magnetic resonance imaging (MRI), X-ray and computational tomography. OCT is useful as a non-invasive diagnostic technique. The axial resolution of OCT is nearly 10~15 μm.

OCT was developed by David Huang in the Optic Group, Research Laboratory of Electronics and Department of Electrical Engineering and Computer Science, M.I.T in 1991. OCT is an extensional technique of optical coherence domain reflectometry (OCDR). OCDR is based on low coherence Michelson interferometer that has a one dimensional ranging where the delay of backscattering from a tissue. OCT was implemented by coupling high speed OCDR system with transverse scanning of probe beam. [45]. OCT employs light from a broadband light source, which is divided into a reference and a sample beam, to obtain a reflectivity versus depth profile of the retina. The light waves that are backscattered from the retina, interfere with the reference beam, and this interference pattern is used to measure the light echoes versus the depth profile of the tissue in vivo.

OCT can be largely separated time-domain OCT (TD-OCT) and Fourier-domain OCT (FD-OCT) as reference mirror movement. Also, FD-OCT can be divided into spectral-domain OCT (SD-OCT) and swept source OCT (SS-OCT). Furthermore, like polarization-sensitive OCT (PS-OCT), Doppler OCT, there are many kinds of OCT in OCT techniques.

2.1.1 Optical coherence tomography (OCT)

Optical coherence tomography (OCT) system measures interference signal between reference arm and sample arm. OCT needs an interferometer because OCT uses optical path difference (OPD) between sample arm and reference arm. Therefore, OCT system can be explained by interferometers of various type such as Michelson and Mach-Zehnder.

Fig. 2-1 shows basic OCT scheme composed by light source, interference part and detection part. The light from source could be delivered to interference part. Next, interference fringe made by OPD could be converted light into electrical signal and be processed in detection part.
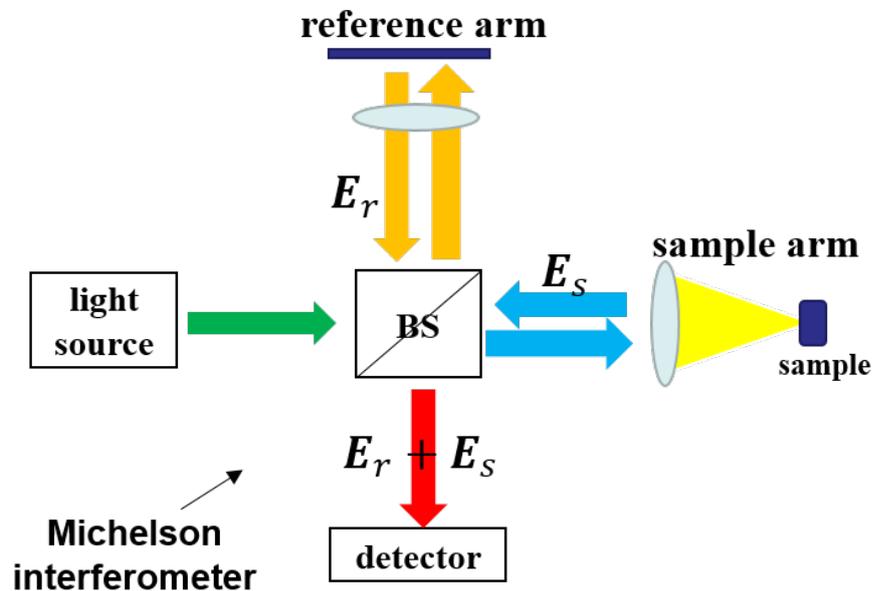
Figure 2-1. Basic OCT scheme using Michelson interferometer.

In this chapter, once interference signal using monochromatic source is explained, the signal using broadband source will be explained.

2.1.2 Interference signal using monochromatic source

Eq. (1) and (2) means reflected electrical field signal from each reference arm and sample arm. Generally, these electrical field can be expressed by Euler's formula because light can be regarded as wave. Here, l_s and l_r are optical path length from beam splitter (BS) to end of each arm. [46]

$$E_r = \beta_R e^{[-j(2k_r l_r - \omega t)]} \quad (1)$$

$$E_s = \beta_S e^{[-j(2k_s l_s - \omega t)]} \quad (2)$$

β_s and β_r are reflectivity, k_r and k_s are propagation constant in each arm. ω is frequency of a light source and t is a travel time from BS to sample and reference arm. In detection part, the interference signal could be calculated by photocurrent equation (3) [46].

$$I = \frac{\eta e}{hv} \left(\frac{|E_r + E_s|^2}{2z_0} \right) \quad (3)$$

Here, η is quantum efficiency, hv is energy of photon and e quantity of electric charge and z_0 is an intrinsic impedance of free space. $|E_r + E_s|^2$ in photocurrent equation can be represented by [46]

$$I = \frac{\eta e}{h v} \left(\frac{1}{\eta_0}\right) \left[\frac{1}{2}|\beta_r|^2 + \frac{1}{2}|\beta_s|^2 + real\{E_s E_r^*\}\right] \quad (4)$$

$$real\{E_s E_r^*\} = \beta_s \beta_r \cos(2k_s l_s - 2k_r l_r)$$

$$= \beta_s \beta_r \cos(2\frac{2\pi}{\lambda}(l_s - l_r)) = \beta_s \beta_r \cos(2\frac{2\pi}{\lambda}(\Delta l)) \quad (5)$$

Here, $real\{E_s E_r^*\}$ can be changed by OPD. In eq. (4), $\frac{1}{2}|\beta_r|^2 + \frac{1}{2}|\beta_s|^2$ term should be eliminated because the DC term have an only light power without reference to OPD. In data processing, the DC term can be regarded as noise. The $real\{E_s E_r^*\}$ (AC term) is used to acquire image in OCT system [46].

2.1.3 Interference signal using broadband source

Generally, most OCT system uses broadband source because the broadband source is better than monochromatic source in resolution. The broadband source can be expressed by frequency summation of monochromatic sources. Therefore, eq. (1), (2) and (5) in previous chapter can be changed by [46]

$$E_r = \beta_r e^{[-j(2k_r l_r - \omega t)]} \rightarrow E_r = \beta_r e^{[-j(2k_r(\omega)l_r - \omega t)]} \quad (6)$$

$$E_s = \beta_s e^{[-j(2k_s l_s - \omega t)]} \rightarrow E_s = \beta_s e^{[-j(2k_s(\omega)l_s - \omega t)]} \quad (7)$$

$$I \propto real\{E_s E_r^*\} \rightarrow real \int_{-\infty}^{\infty} E_S(\omega) E_R^*(\omega) \frac{d\omega}{2\pi} \quad (8)$$

Here, according to Wiener-Khintchin theorem, power spectral density of the light source and interference fringe in photo current are Fourier transform relationship. Therefore, eq. (8) could be changed by Wiener-Khintchin theorem [46]

$$I \propto real \int_{-\infty}^{\infty} E_s(\omega)E_r^*(\omega) \frac{d\omega}{2\pi} \rightarrow real \int_{-\infty}^{\infty} S(\omega)e^{[-j\Delta\varphi(\omega)]} \frac{d\omega}{2\pi}$$

$$S(\omega) = \beta_s(\omega)\beta_r^*(\omega), \ \Delta\varphi(\omega) = 2k_s(\omega)l_s - 2k_r(\omega)l_r. \tag{9}$$

$S(\omega)$ is an equation of frequency spectrum of the light source and $\Delta\varphi(\omega)$ is phase difference in detection part.

If sample arm and reference arm are uniformed, non-dispersive medium and the center wavelength of the light source is ω_0 and frequency spectrum is $S(\omega - \omega_0)$, the propagation constant $k(\omega)$ can be represented by 1st Taylor's series as followed [46],

$$k_s(\omega) = k_r(\omega) = k(\omega_0) + k'(\omega_0)(\omega - \omega_0) \tag{10}$$

In this case, $\Delta\varphi(\omega)$ is also changed by Δl (OPD)

$$\Delta\varphi(\omega) = 2k_s(\omega)l_s - 2k_r(\omega)l_r$$

$$= 2[k(\omega_0) + k'(\omega_0)(\omega - \omega_0)]l_s - 2[k(\omega_0) + k'(\omega_0)(\omega - \omega_0)]l_r$$

$$= 2k(\omega_0)\Delta l + 2k'(\omega_0)(\omega - \omega_0)\Delta l \tag{11}$$

9

Finally, eq. (9) can be represented by

$$I \propto real\{e^{[-j\omega_0\Delta\tau_p]} \int_{-\infty}^{\infty} S(\omega - \omega_0)e^{[-j(\omega-\omega_0)\Delta\tau_g]} \frac{d(\omega-\omega_0)}{2\pi} \quad (12)$$

Here, $\Delta\tau_g$ and $\Delta\tau_p$ are group velocity and phase velocity as followed

$$\Delta\tau_p = \frac{k(\omega_0)}{\omega_0}(2\Delta l) = \frac{2\Delta l}{v_p} \quad (13)$$

$$\Delta\tau_g = k'(\omega_0)(2\Delta l) = \frac{2\Delta l}{v_g} \quad (14)$$

The interference signal of photocurrent is composed of fast part and envelop part. In eq. (12) and fig. 2-2 , first term means phase velocity and second integral term means group velocity [46].
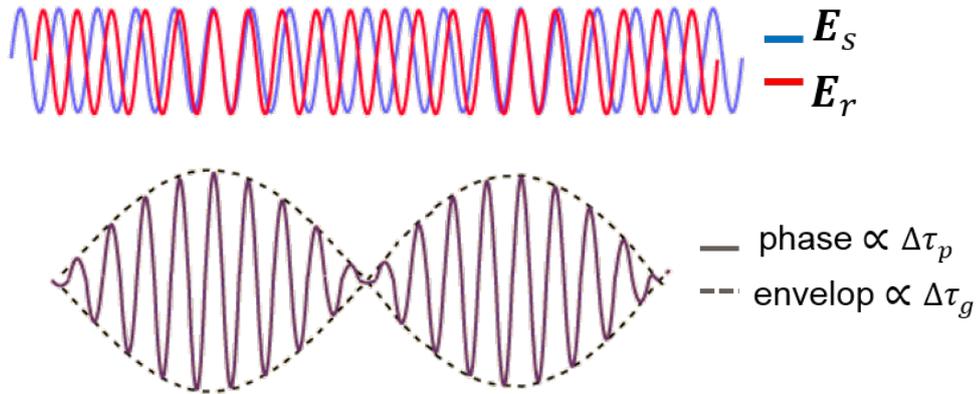
Figure 2-2. Detection of interference signal.

Next, assume that the light source has Gaussian shape, $S(\omega)$ can be represented by

$$S(\omega) = \beta_s(\omega)\beta_r^*(\omega) = \frac{2\sqrt{\ln 2}}{\sqrt{\pi}\Delta\omega} e^{\left[-4\ln 2(\frac{\omega-\omega_0}{\Delta\omega})^2\right]} \qquad (15)$$

Continuously, eq. (12) can be represented by using eq. (15) as followed,

$$I \propto e^{\left[-(\frac{\sqrt{\pi}}{2\sqrt{\ln 2}}\frac{\Delta\lambda}{\lambda_0^2}\Delta l)^2\right]} \cos(2\frac{2\pi}{\lambda_0}\Delta l) \qquad (16)$$

In eq. (16), exponential term means envelop of interference signal and cosine term indicate phase velocity changed by Δl. The $\frac{\Delta\lambda}{\lambda_0^2}$ represents bandwidth of the light source.

2.1.4 Swept source OCT (SS-OCT)

TD-OCT is already applied as a medical diagnostics in 1990s. In spites of success in medical diagnostics, TD-OCT has disadvantages which are relatively complex optical and mechanical alignment needed to scan ~10ps delays at kHz rates to acquire real-time imaging [47].

In order to overcome those of TD-OCT, it needs to an interferometric signal with minimized scanning time at a fixed delay of each arm. The beginning of FD-OCT has been developed by Fercher et al. in 1995 [48]. This methods can be divided into two kinds spectral discrimination (SD) and swept source (SS) OCT. While SD-OCT uses super-luminencent diode

(SLD) broadband source, diffraction grating and spectrometer to acquire real-time imaging, SS-OCT uses swept source laser without spectrometer and diffraction grating.

Again, the nth photodetector output is represented by

$$P_n(k) = |E_r + E_s|^2 \cong 2S(k)\sqrt{\beta_r\beta_s}\cos(2k\Delta l) \qquad (17)$$

k is a wavenumber, $S(k)$ is an equation of frequency spectrum of the light source (watts per wavenumber), Δl is OPD. In the case of SS-OCT, $k = k_0 + t(\Delta k/\Delta t)$,where t is time, k_0 is an initial wavenumber, and Δt is the sweep (A-scan time) and Δk is the bandwidth of the swept source, thus [47]

$$D_n[K] = \frac{1}{2^n}\rho S(K)\sqrt{\beta_r\beta_s}\cos(2K\Delta l) \qquad (18)$$

Where, $K = \{k_1, k_2, \dots, k_M\}$, ρ is the detector responsivity and $S(K)$ is the illuminated power of sample. The purpose of SS-OCT is to get the depth profile $D[l]$ of the sample arm ($l = \pm\Delta l$) [47].

$$D[l] = \sum_{m=1}^{M} D_n[K]\exp[-j2Kl] \cong \frac{1}{2}\rho\sqrt{\beta_r\beta_s}\sum_{m=1}^{M} S(K)$$

$$= \frac{1}{2}\rho\sqrt{\beta_r\beta_s}S_{SS-OCT} \qquad (19)$$

S_{SS-OCT} is the total summation of $S(K)$. is the detector responsivity and $S(K)$ is the illuminated power of sample. The purpose of SS-OCT is to get the depth profile $D[l]$ of the sample arm [47].

2.1.5 Common-path OCT in SMART system

Conventional OCT of Michelson type has several disadvantages. Optical alignment in Michelson interferometer requires complicate tasks.

In this study, OCT is used to distance sensor composed of optical fiber in Fig. 2-3. The OCT distance sensor in dual SMART system should be lighten and flexible to provide surgeons with convenience. Fig. 2-3 means common-path interferometer. Reference arm and sample arm share their optical path until end of optical fiber.

The difference of refractive index between optical fiber and air make reference arm. Here, Δl is changed by hand tremor. In detection part, Δl by hand tremor can be analyzed.
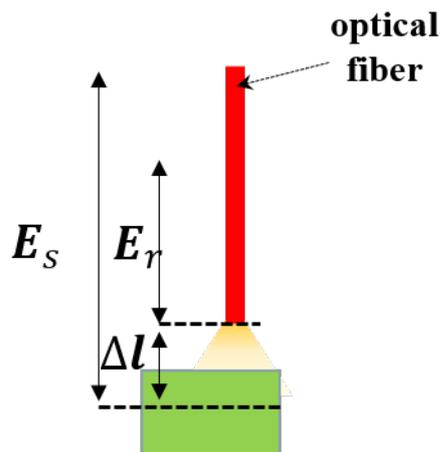
Figure 2-3. Common-path interferometer

3. DESIGN OF DUAL SMART SYSTEM

3.1 SMART horizontal micro-forceps and scissors

We introduced microsurgery with OCT in previous chapter. To study the precise and safe micro-surgical manipulator, the SMART system can be largely divided into 'sensing part' and 'actuating part'. The OCT is used as a distance sensor thanks to its high axial resolution.

The physiological hand tremor of micro-surgeons was approximately 6-12 Hz with unintended sinusoidal motion of 100 μm. In the sensing parts of the SMART system, the axial resolution of OCT was 5-15 μm, it is enough to detect the amplitude of hand tremor. In this study, CP SS-OCT distance sensor was used.

3.1.1 System specification

The swept source laser is consisted of a OEM engine (AXSUN, $\lambda_0=\mathbf{1060\ nm}$, sweeping rate = 100 kHz, 3 dB axial resolution = 8 μm, scan range = 3.7 mm in air), a detector and a digitizer with 500 MSPS (12 bit resolution), a frame grabber (National Instruments), a computer, and PZT motor (LEGS-LL1011A) with a motor controller (PMD101, 125 kHz) in fig. 3-1 and fig. 3-2.
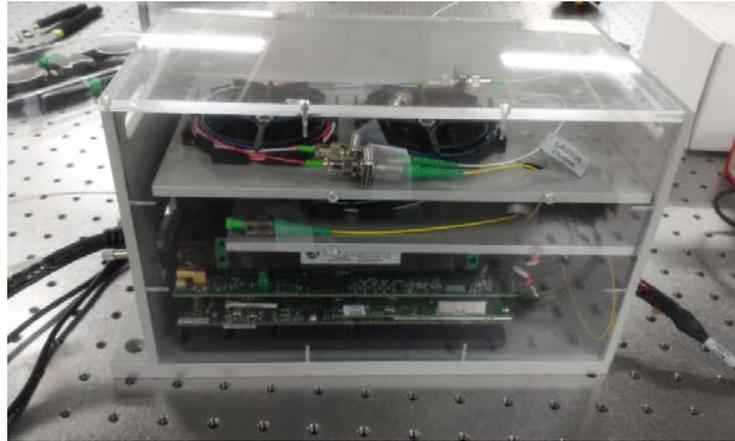
Figure 3-1. The swept source OCT OEM engine.

Figure 3-2. The PZT motor.

The compensation system is composed of two PZT motors (LEGS-LL1011A, 22 mm $\times$10.8 mm $\times$ 18.7 mm) and two controllers (PMD 101). The PZT motor has 0-15mm/s of speed range and 6.5N force. The motor controller can detect 2048 μsteps/wfm-step. To compensate hands tremor efficiently, each height error between desired height and actual height is compensated as system rate of 500 Hz after set the desired height [27].

3.1.2 Dual SMART system

To detect and compensate the height variations by tremor of both hands, it is followed as fig. 3-3. Detection of the tremor of both hands is performed by two OCT distance sensors in each end-effector. OCT distance sensor system consists of SS-OCT engine (center wavelength = 1060 nm, axial resolution = 8 μm, AXSUN), three fused couplers, two detectors and a digitizer (sampling rate = 500 MSPS (12 bit resolution)). The OCT sensor system could be lightened because the sensors are operated by only a light source. Once the reflected OCT signal from target surface is transmitted to the computer (i7 3.4 GHz) through the digitizer of 500 Mbps, it could provide height of each end-effector with micro-surgeons. On simultaneous grasping and dissecting tasks, height of a micro-forceps should higher than a micro-scissors. In consideration of coherence length (3 mm) of OCT source, the active height of each end-effector could be set systematically. Thereby, the system could provide active guidance to the sample with each end-effector. To obtain a clear OCT distance signal with high signal-to-noise-ratio (SNR) in vivo, OCT distance sensor is combined with ball-lens. When OCT distance sensor (n=1.464) is directly used to measure the hands tremor, it may have very low SNR reflected signals because the refractive index of inner body (n=1.33) is close to that of OCT sensors [27].
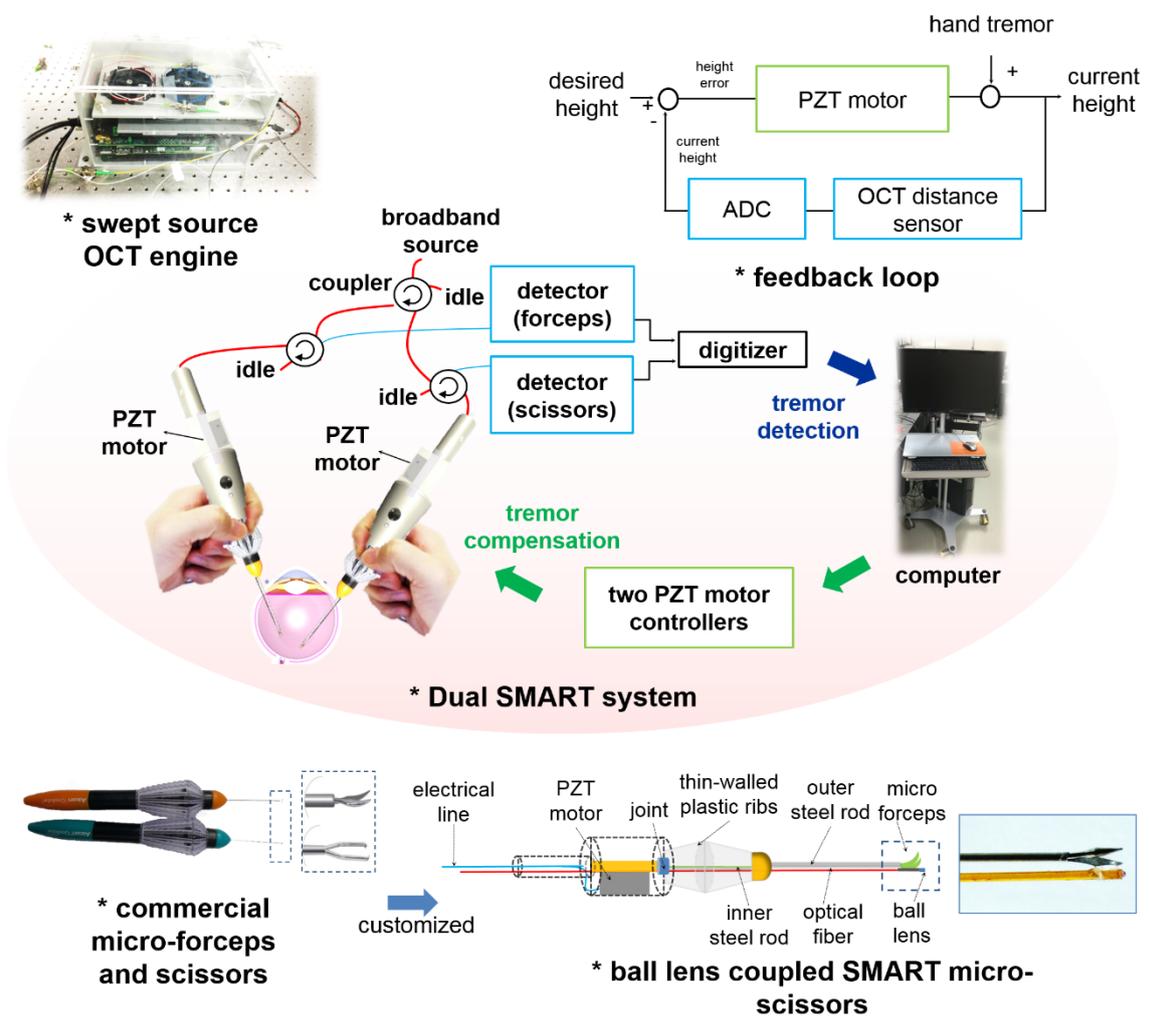
Figure 3-3. Dual SMART system. Each instrument are combined with ball lens to increase SNR

Fig 3-4. shows the comparison of SNR between ball lens coupled OCT and a bare fiber signal on a paper. The amplitude of ball-lens did not show a remarkable decrease without reference to tilted angle of the end-effector. The SNR of the ball-lens coupled OCT distance sensor is higher than that of bare fiber approximately 1.3 times because ball-lens could focus the beam. Also, it is highly difficult to apply the actual surgeon's task due to low numerical aperture (NA= 0.14, 8 degree). In other words, micro-surgeons could not tilt micro-surgical instruments over 8 degree. In actual micro-surgical tasks, however they cannot help but be tilted over 8 degree. The system could operate over 45 degree by using a ball-lens [27].
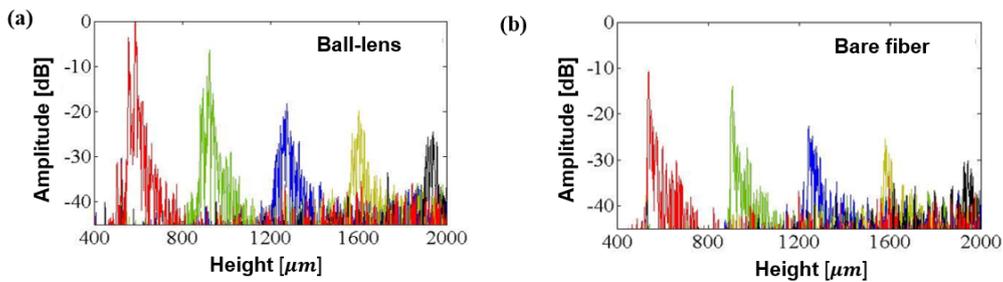
Figure 3-4. Comparison between ball-lens coupled OCT sensor and bare fiber OCT sensor
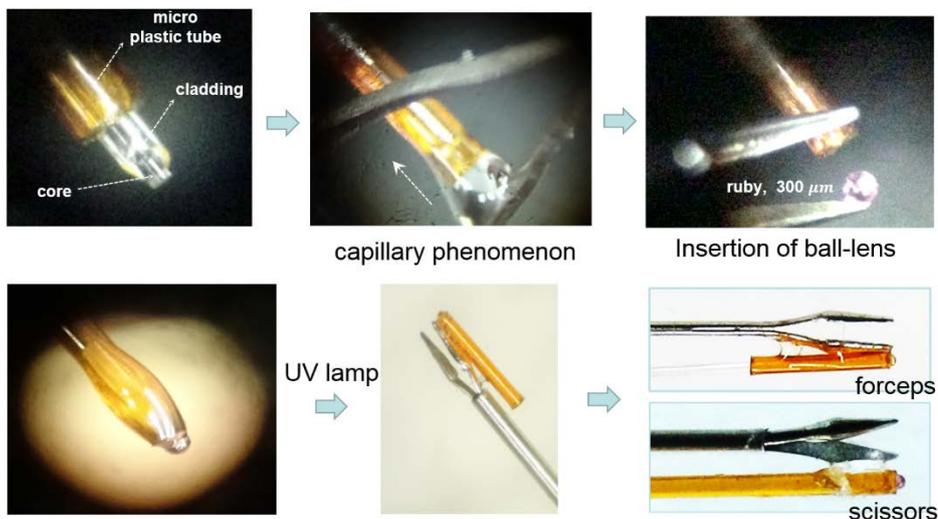
Figure 3-5. Ball lens coupled micro forceps manufacturing procedure.

3.2 Implementation of SMART horizontal scissors and forceps

3.2.1 SMART horizontal micro-scissors system

The horizontal micro-scissors is useful to delaminate the retinal detachment and segmentation. Compared to the blade, surgeons incise the surgical sample by rotating the tool along the tool axis, scissors is greatly useful. Additionally, horizontal-micro-scissors is developed to dissect the surgical target which is lengthen vertically. It could be made by attaching 20 gauge commercial syringe needle (20-gauge and 25-gauge, BD syringe) to the scissors and its linear motion could be converted into horizontal motion in Fig. 3-8 [26].
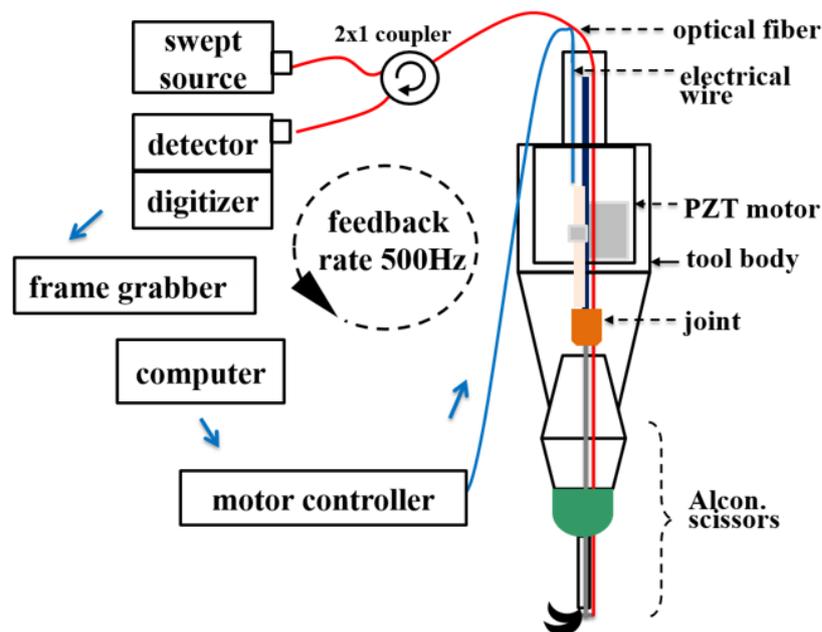
Figure 3-6. The Schematic of the CP SS-OCT guided horizontal SMART micro-scissors.
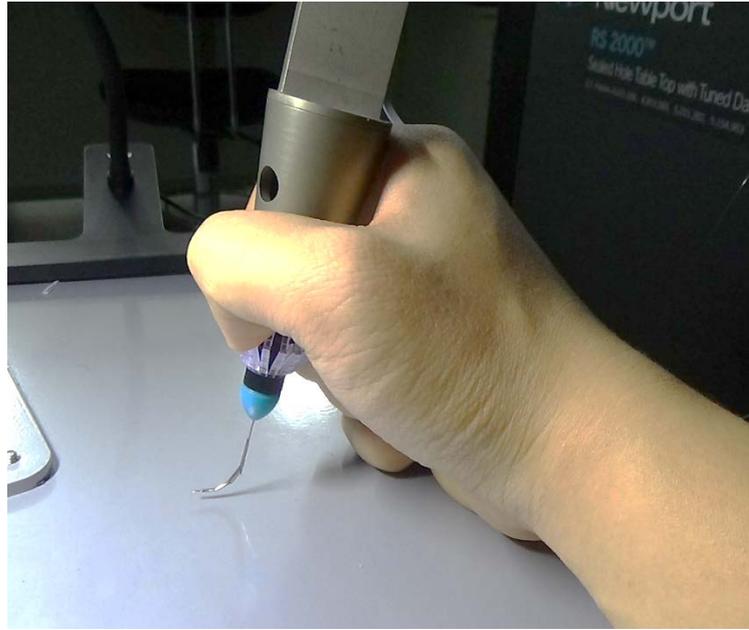
Figure 3-7. Actual image corresponding to horizontal micro-scissors system.

optical
fiber

micro
plastic tube

ball lens

(a)

① ② ③

Original commercial scissors.

(b)

①

cut the blue
square area

(c)

②

make a hole

(d)

③

bend the inner needle
20 gauge steel tube

(e)

attach the 20 gauge
steel tube to the inner
needle.
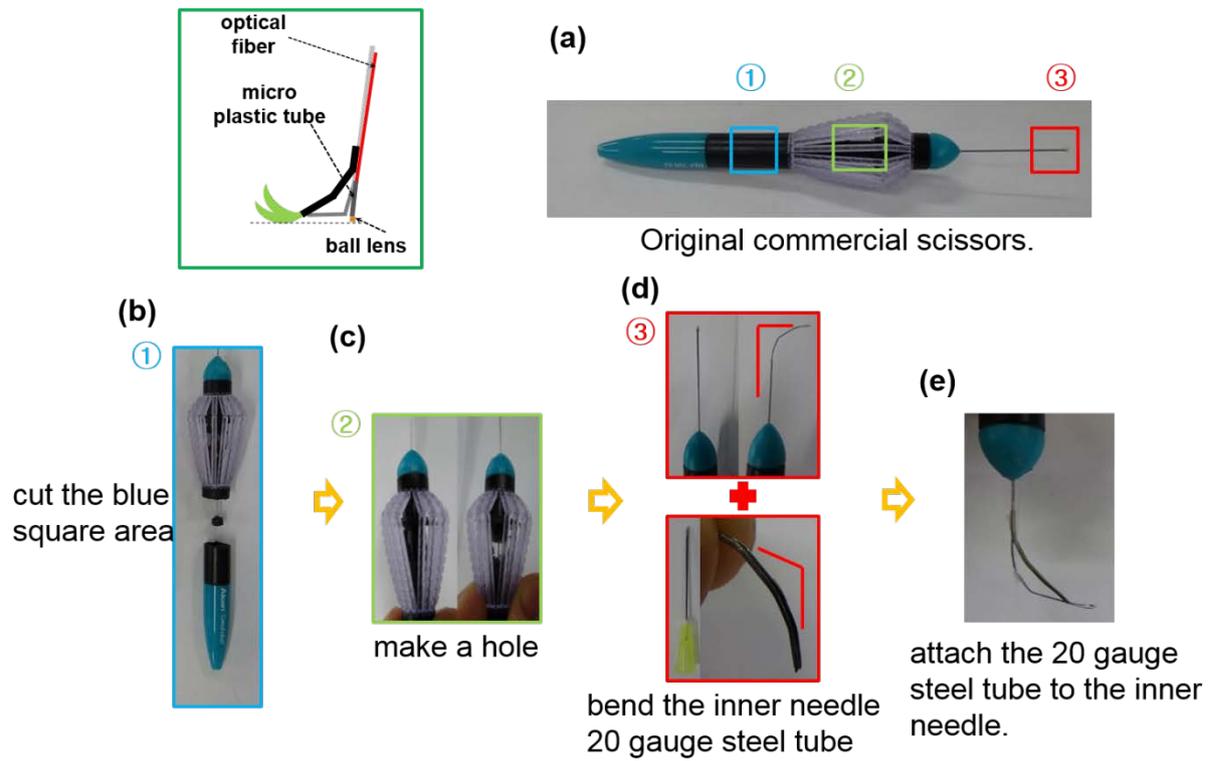
Figure 3-8. Customizing procedure of horizontal scissors.
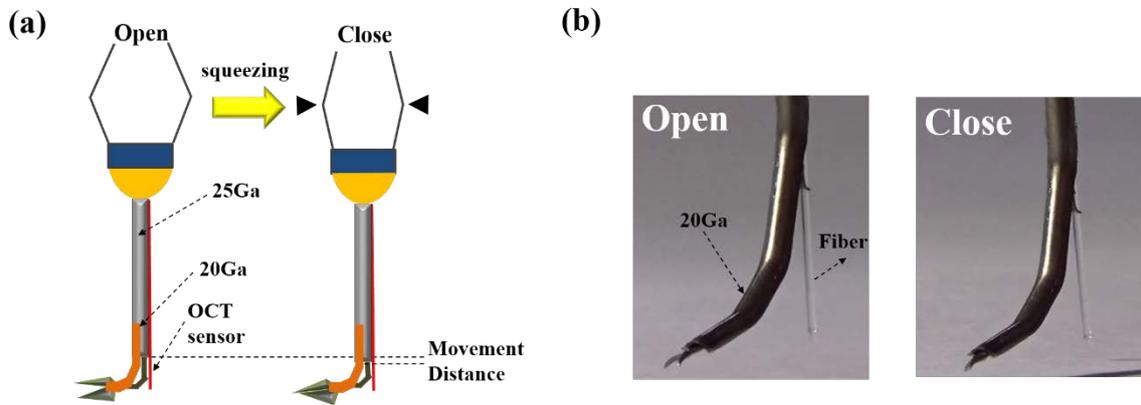
Figure 3-9. Concept of the horizontal dissection. (a) Schematic of the horizontal SMART micro-forceps. (b) Photos of the dissection on dry phantoms.
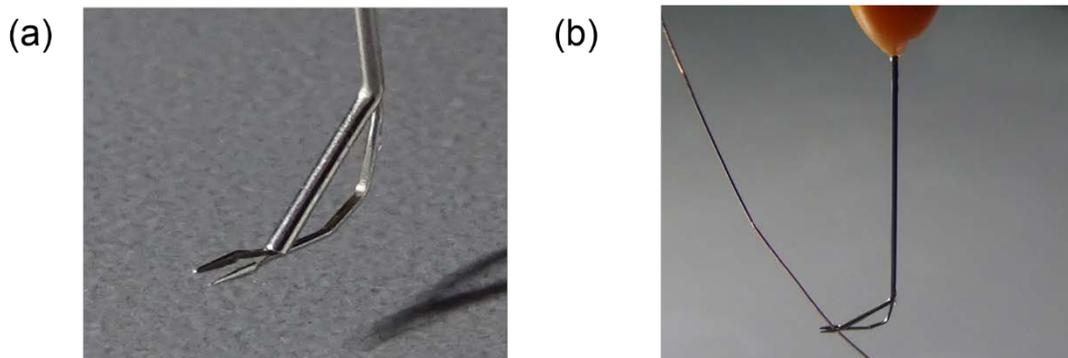
Figure 3-10. Horizontal micro-forceps (a) Actual image corresponding to horizontal scheme. (b) Grasping an electrical line core.

4. EXPERIMENTS

4.1 Hand tremor cancellation in water

In order to adjust the SMART system into biological sample, the hand tremor compensation should be possible in water because most biological samples are aqueous. Also, hand tremor compensations at various angles could be evaluated because previous OCT distance sensor has very low numerical aperture of optical fiber.

Fig. 4-1 shows compensation of hand tremor at various angle in water. The SMART system could maintain the height of its end-effector.
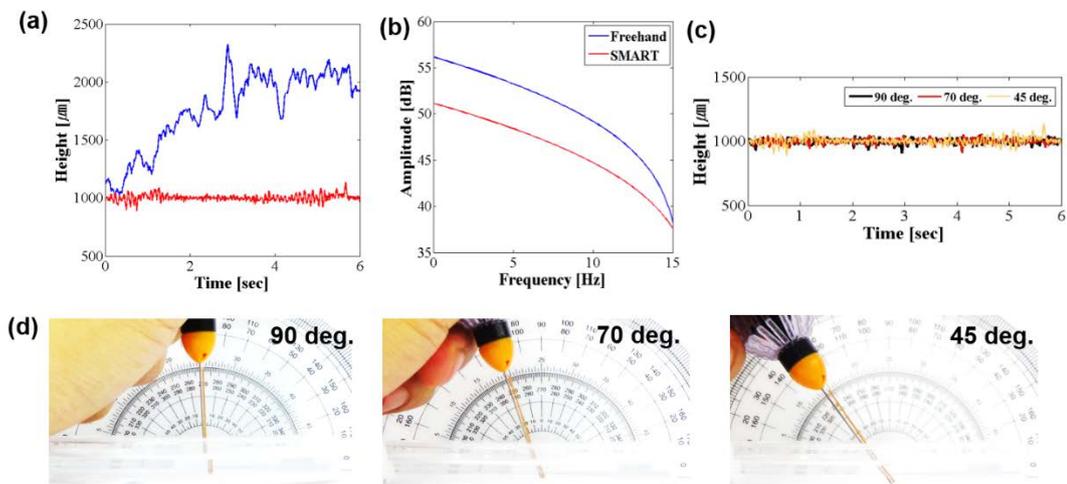
Figure 4-1. Hand tremor compensation at various angles. (a) Height signal comparison between SMART and freehand. (b) Fourier analysis corresponding to (a). Tremor compensation from 90 to 45 deg. (d) Photos of the hand tremor compensation at various angle 90 to 45 deg.

4.2 Bimanual dissection using a biological membrane

Bimanual surgical dissection requires that one hand grasp and stabilize the tissue thereby optimally exposing the target to be incised. Hand tremor during freehand surgery is physiologically unavoidable. In bimanual procedures, the tremor from two hands acting cooperatively must be managed effectively in order to gain the advantages that bimanual surgery provides. Fig. 4-2 shows two surgical situations. In Fig. 4-2(a), a one-handed dissection attempt results in difficult access to the surgical target and lack of precision in the incision made. During bimanual surgery, fixation of the target and exposure of the desired surgical target to the tips of the scissors allows a precise surgical dissection to be made [27].
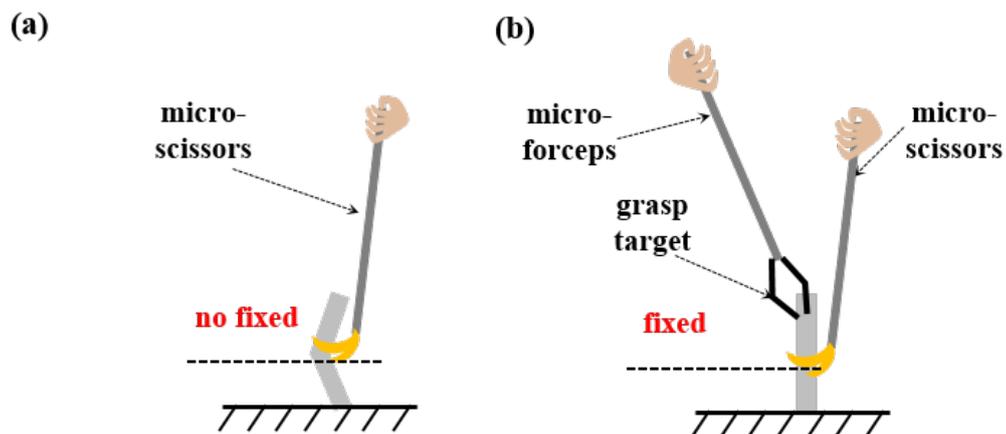
Figure 4-2. Limitation of one-handed dissection. (a) Difficulty of one-handed dissection.

(b) Better performance of bimanual dissection.

Fig 4-3. demonstrates the bimanual dissection of the egg membrane. Each height of end-effector are 2000 micron (forceps) and 1000 micron (scissors). Fig 4-3(a) shows height variations of them. The bimanual SMART system could prove that it has better performance than freehand case in dissection test and completion time. Originally, the freehand case could not achieve accurate dissection because the freehand could not simultaneous task such as, grasping and dissection. Also, it requires more time to find the dissecting point. However, in the case of bimanual manipulation, it has shortest completion times because the target could be fixed by the compensation algorithm. Therefore, the bimanual micro-surgical system could precisely and safely dissect the targets.
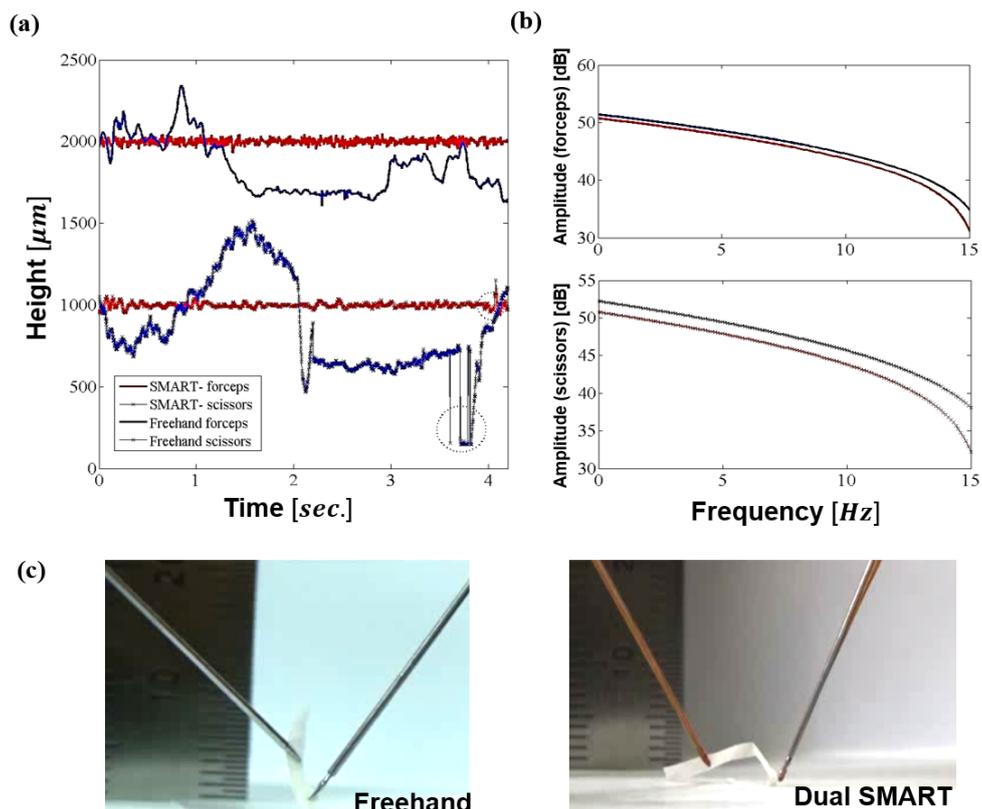
Figure 4-3. The membrane dissection result of height signal comparison between SMART horizontal scissors and freehand.

4.3 Bimanual tasks using a porcine eye

Figure 4-4(a) shows height variations of SMART assisted end-effectors in ex-vivo sample. The sample is a cadaver porcine eye within 3 hours. The bimanual SMART system could maintain each desired height (scissors: 800 μm, forceps: 2000 μm). In 2 times grasping and dissection tasks, the system could rapidly return to the each desired height. Figure 4-4(b) demonstrates actual grasping and dissection tasking media of the bimanual SMART system. Intuitively, stable motion of each end-effector could be observed.

Additionally, in the case of bimanual performance, the RMSE (scissors: 34.15, forceps: 27.98) were higher than previous SMART results because the target surface in porcine eye was not uniform compared to dry phantom. In other words, the more accurate manipulation are required during bimanual tasks. However, the RMSE of the bimanual SMART were still smaller than freehand cases (scissors: 265.66, forceps: 213. 85) because the PZT motor could diminish the hand tremor thanks to the high SNR by ball-lens coupled OCT distance sensor. Therefore, the system could compensate the both hand tremor in biological tissues.

(a)

(b)
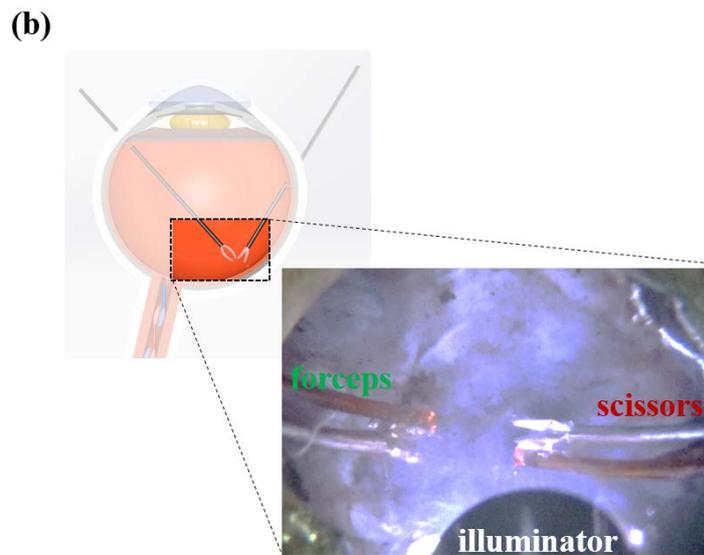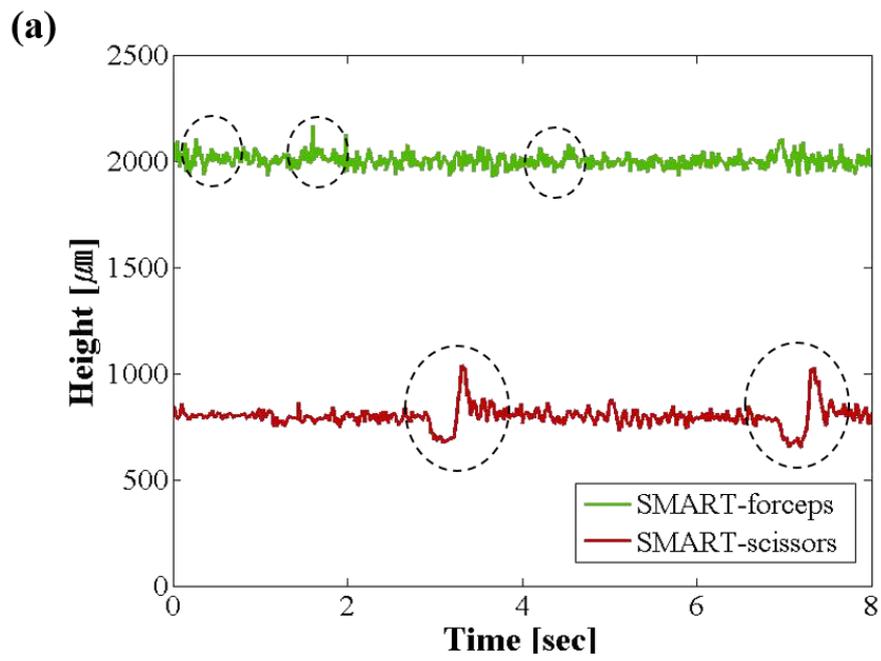
Figure 4-4. The bimanual tasks results in porcine eye.

5. CONCLUSION

Manipulation of micro-surgical tools requires minimized physiological tremor and flexible conversion of surgical tools for specific surgical situation such as bimanual scheme.

In this study, we study the novel dual SMART micro-surgical system to achieve precise bimanual vitrectomy. The dual SMART micro-surgical systems have been developed to suppress the hand tremor and achieve horizontal dissection of surgical target.

The development of dual SMART micro-surgical systems could be divided into elimination of tremor in both hands, improvement of previous optical coherence tomography (OCT) distance sensor using ball-lens and customization of commercial micro-surgical tools for horizontal dissection.

The dual SMART system is consisted of OCT sensor and piezoelectric (PZT) motor built-in each surgical tools. The volume of system could be lightened and developed with reasonable price because two sensors could be made by only one light source. The asynchronous tremor in both hands of 6-12 Hz could be cancelled by feedback rate of 500 Hz. From bimanual dissection of an egg membrane, the dual SMART system proved that the system could compensate the tremor in both hands effectively. During membrane dissection, this system could maintain the desired height of each surgical tools than freehand. Also, the dual SMART system could reduce the hand tremor in *ex-vivo*.

The ball-lens coupled OCT distance sensor could detect the hand tremor at various angles thanks to its spherical shape. Additionally, high numerical aperture (NA) of ball-lens provide high signal-to-ratio (SNR) better than bare fiber based OCT distance sensor. Therefore, the ball-lens coupled OCT sensor is more suitable for aqueous biological sample.

The SMART horizontal micro-scissors could provide surgeons with comfortable horizontal dissection and reduced hand tremor through customization.

In the future, the dual SMART system will be innovate micro-surgical system with ergonomic design in microsurgery.

REFERENCES

[1]   J. U. Kang, J. H. Han, X. Liu, K. Zhang, C. G. Song, P. Gehlbach, "Endoscopic functional fourier domain common path optical coherence tomography for microsurgery," IEEE J. Sel. Top Quantum Electron 16(4), 781-792 (2010).

[2].   J. U. Kang, Y. Huang, K. Zhang, Z. Ibrahim, J. Cha, W. P. Lee, Brandacher G, Gehlbach PL, "Real-time three-dimensional Fourier-domain optical coherence tomography video image guided microsurgeries," J. Biomed. Opt. 17(8) 081403-1 (2012).

[3].   J. U. Kang, Y. Huang, K. Zhang, Z. Ibrahim, J. Cha, A. W. P. Lee, G. Brandacher, and P. L. Gehlbach, "Real-time three-dimensional Fourier-domain optical coherence tomography video image guided microsurgeries," J. Biomed. Opt 17(8) 081403–1–6 (2012).

[4].   M. Balicki, R. Richa, M. Balicki, B. Vagvolgyi, P. Kazanides, P. Gehlbach, J. Handa, J. Kang, R. Taylor, "Interactive OCT annotation and visualization for vitreoretinal surgery" Augmented Environments for Computer-Assisted Interventions. Lecture Notes in Computer Science. 7815, 142-152 (2013).

[5].   C. N. Riviere, J. Gangloff, and M. Mathelin, "Robotic Compensation of Biological Motion to Enhance Surgical Accuracy," in Proceedings of IEEE 94(9), 1705–1716 (2006).

[6].   B. C. Becker, R. A. MacLachlan, L. A. Lobes, Jr., and C. N. Riviere, "Semiautomated intraocular laser surgery using handheld instruments," Lasers Surg. Med. 42(3), 264–273 (2010).

[7].   W. T. Latt, U. X. Tan, C. Y. Shee, and W. T. Ang, "A compact hand-held active physiological tremor compensation instrument," in Proceedings of IEEE Conference on Advanced Intelligent Mechatronics (IEEE, 2009), pp. 711–716.

[8].   R. A. MacLachlan, B. C. Becker, J. C. Tabarés, G. W. Podnar, L. A. Lobes, and C. N. Riviere, "Micron: An actively stabilized handheld tool for microsurgery," IEEE Trans. Robot 28(1), 195–212 (2012).

[9].   Yang, S, R. A. MacLachlan, and C. N. Riviere, "Manipulator design and operation of a six-degree-of-freedom handheld tremor-canceling microsurgical instrument," IEEE/ASME Trans. Mechatron., 1–12 (2014).

[10].   R. Taylor, P. Jensen, L. Whitcomb, A. Barnes, R. Kumar, D. Stoianovici, P. Gupta, Z. Wang, E. de Juan, Jr., and L. Kavoussi, "A steady-hand robotic system for microsurgical augmentation," Int. J. Robot. Res 18(12), 1201–1210 (1999).

[11.   Z. Sun, M. Balicki, J. Kang, J. Handa, P. Gehlbach, R. Taylor, and I. Iordachita, "A Sub-Millemetric, 0.25 mN Resolution Fully Integrated Fiber-Optic Force Sensing Tool for Retinal Microsurgery,"   Int. J. Comput. Assist Radiol. Surg. 4(4) 383–390 (2009).

[12].   A. Uneri, M. Balicki, J. Handa, P. Gehlbach, R. Taylor, and I. Iordachita, "New steady-hand eye robot with micro-force sensing for vitreoretinal surgery," in Proceedings of IEEE BioRob., 814–819 (2010).

[13].   M. Balicki, A. Uneri, I. Iordachita, J. Handa, P. Gehlbach, and R. Taylor, "Micro-force Sensing in Robot Assisted Membrane Peeling for Vitreoretinal Surgery," Med. Image. Comput. Comput. Assist. Interv., 13(Pt 3), 303–310 (2010).

[14]   X. Liu, M. Balicki, R. H. Taylor, and J. U. Kang, "Towards automatic calibration of Fourier-Domain OCT for robot-assisted vitreoretinal surgery," Opt. Express 18(23), 24331–24343 (2010).

[15]   R. Taylor, J. U. Kang, I. Iordachita, G. Hager, P. Kazanzides, C. N. Riviere, E. Gower, R. Richa, M. Balicki, X. He, X. Liu, K. Olds, R. Sznitman, B. Vagvolgyi, P. L. Gehlbach, and J. Handa, "Recent work toward a microsurgical assistant for retinal surgery," in Hamlyn Symposium on Medical Robotics, 3-4 (2011).

[16]   X. He, D. Roppenecker, D. Gierlach, M. Balicki, K. Olds, P. L. Gehlbach, J. Handa, R. Taylor, and I. Iordachita, "Toward clinically applicable steady-hand eye robot for vitreoretinal surgery," in Proceedings of International Mechanical Engineering Congress and Exposition, 145-153 (2012).

[17]   X. He, J. Handa, P. Gehlbach, R. Taylor, I. Iordachita, "A sub-millimetric 3-DOF force sensing instrument with integrated fiber Bragg grating for retinal microsurgery," IEEE Trans. Biomed. Eng. 61(2) 522–534 (2014).

[18]   N. Cutler, M. Balicki, M. Finkelstein, J. Wang, P. Gehlbach, J. McGready, I. Iordachita, R. Taylor, J. T. Handa, "Auditory force feedback substitution improves surgical precision during simulated ophthalmic surgery," Invest. Ophthalmol. Vis. Sci. 54 (2) 1316-24 (2013).

[19]   B. Gonenc, J. Handa, P. Gehlbach, R. Taylor, and I. Iordachita "A Comparative Study for Robot Assisted Vitreoretinal Surgery: Micron vs. the Steady-Hand Robot," in Proceedings of IEEE Conference on Robotics and Automation (IEEE, 2013), pp. 4832 -4837.

[20]   B. Gonenc, N. Tran, C.N. Riviere, P. Gehlbach, R.H. Taylor, and I. Iordachita, "Force-Based Puncture Detection and Active Position Holding for Assisted Retinal Vein Cannulation," in Proceeding of IEEE International Conference on Multisensor Fusion and Information Integration (IEEE 2015), pp. 322-327.

[21]   C. Song, P. L. Gehlbach, and J. U. Kang, "Swept source optical coherence tomography based smart handheld vitreoretinal microsurgical tool for tremor suppression," in Proceedings of IEEE Conference on Engineering Medicine and Biology Society (IEEE, 2012), pp.1405-1408.

[22]   C. Song, P. L. Gehlbach, and J. U. Kang, "Active tremor cancellation by a 'smart' handheld vitreoretinal microsurgical tool using swept source optical coherence tomography," Opt. Express 20(21), 23414–23421(2012).

[23]   C. Song, P. L. Gehlbach, and J. U. Kang, "Ball lens fiber optic sensor based smart handheld microsurgical instrument," Proc. of SPIE 8576: 857601 (2013).

[24]   C. Song, D. Y. Park, P. L. Gehlbach, and J. U. Kang, "Fiber-optic OCT sensor guided "SMART" micro-forceps for microsurgery," Biomed. Opt. Express 4(7), 1045-1050(2013).

[25]   C. Song, P. L. Gehlbach, and J. U. Kang, "CP-OCT sensor guided SMART micro-forceps," Proc. of SPIE 8938: 893814 (2014).

[26]   H. C. Park, C. B. Yeo, and C. song, "SMART micro-scissors based precise incision" Proc. of SPIE 9317: 93170 (2015).

[27]   H. C. Park, C. B. Yeo, P. L. Gehlbach, and C, Song, "Development of the Dual Smart Micro-surgical System using Common-path Swept Source Optical Coherence Tomography," in Proceedings of IEEE Conference on Engineering Medicine and Biology Society (IEEE, 2015), pp. 5-8.

[28]   K. Zhang, W. Wang, J. H. Han, and J. U. Kang, "A surface topology and motion compensation system for microsurgery guidance and intervention based on common-path optical coherence tomography," IEEE Trans. Biomed. Eng 56(9), 2318–2321 (2009).

[29]   K. M. Joos and J.-H. Shen, "Miniature real-time intraoperative forward-imaging optical coherence tomography probe," Biomed. Opt. Express 4(8), 1342–1350 (2013).

[30]   J. P. Ehlers, T. Tam, P. K. Kaiser, D. F. Martin, G. M. Smith, and S. K. Srivastava, "Utility of intraoperative optical coherence tomography during vitrectomy surgery for vitreomacular traction syndrome," Retina 34(7) 1341–1346 (2014).

[31]   J. P. Ehlers, S. K. Srivastava, D. Feiler, A. I. Noonan, A. M. Rollins, and Y. K. Tao, "Integrative Advances for OCT-Guided Ophthalmic Surgery and Intraoperative OCT: Microscope Integration, Surgical Instrumentation, and Heads-Up Display Surgeon Feedback," PLoS One 9(8) (2014).

[32]   Y. K. Tao, S. K. Srivastava, and J. P. Ehlers, "Microscope-integrated intraoperative OCT with electrically tunable focus and heads-up display for imaging of ophthalmic surgical maneuvers," Biomed. Opt. Express 5(6) 1877–1885 (2014).

[33]   C. J. Payne, H. J. Marcus, and G.-Z. Yang, "A Smart Haptic Hand-Held Device for Neurosurgical Microdissection," Ann. Biomed. Eng 43(9), 2185-2195 (2015).

[34]   H. Yu, J.-H. Shen, R. J. Shah, N. Simaan, and K. M. Joos, "Evaluation of microsurgical tasks with OCT-guided and/or robot-assisted ophthalmic forceps," Biomed. Opt. Express 6(2), 457–472 (2015).

[35]   X. Liu, I. I. Iordachita, X. He, R. H. Taylor, and J. U. Kang, "Miniature fiber-optic force sensor based on low-coherence Fabry-Pérot interferometry for vitreoretinal microsurgery," Biomed. Opt. Express 3(5), 1062–1076 (2012).

[36]   G. W. Cheon, Y. Huang, J. Cha, P. Gehlbach, J. U. Kang, "Accurate real-time depth control for CP-SSOCT distal sensor based handheld microsurgery tools," Biomed. Opt. Express 6(5) 1942-1953 (2015).

[37]   K. Zhang and J. U. Kang, "Common-path low-coherence interferometry fiber-optic sensor guided microincision," J. Biomed. Opt 16(9), 095003 (2011).

[38]   H. Fine, R. S. Hoffman, and M. Packer, "Optimizing refractive lens exchange with bimanual microincision phacoemulsification", J Cataract Refract Surg, 30(3):550–554(2004)

[39]   E. Sohn, U. scott, and D. Eliott, "Bimanual Vitreoretinal Surgery for Tractional Retinal Detachment Due to Proliferative Diabetic Retinopathy", Retina Today, 41-43 (2011)

[40]   M. Horiguchi, Y. Kojima, Y. Shimada, "New system for fiberoptic-free bimanual vitreous surgery", Arch Ophtalmol, 120(4), pp. 491-494 (2002).

[41]   E. Burdet, R. Gassert, F. Mani, F. Wang, C. L. Teo, H. Bleuler, "Design of a haptic forceps for microsurgery training" Proc. Eurohaptics (2004).

[42]   Y. Horise, X. He, P. Gehlbach, R. Taylor, I. Iordachita, "FBG-Based Sensorized Light Pipe for Robotic Intraocular Illumination Facilitates Bimanual Retinal Microsurgery," in Proceedings of IEEE Conference on Engineering Medicine and Biology Society (IEEE, 2015), pp. 13-16.

[43]   M. G. Yaşargil, M. Curcic, and C. D. Abernathey. Microneurosurgery. Thieme, "Microneurosurgery," (1996)

[44]   Mohamed M. A Lolah, Ashraf S shaarawy, "A comparative stufy of 23 G vitrectomy and bimanual surgery in the management of epiretinal membranes in diabetic eyes," J. Egyptian Ophthalmological Society 107(4) pp.214-219, (2014)

[45]   D. Huang, E. A. Swanson, C. P. Lin, J. S. Schuman, W. G. Stinson, W. Chang, ... & C. A. Puliafito,. "Optical coherence tomography," *Science*, 254(5035), pp. 1178-1181, (1991)

[46]   M. E. Brenzinski, "Optical coherence tomography:principle and Applications," Elsevier, chapter 3-5 (2006)

[47]   M. A. Choma, M. V. Sarunic, C. Yang, and J. Izatt, "Sensitivity advantage of swept source and Fourier domain optical coherence tomography," *Opt. Express* 11, 2183–2189 (2003).

[48]   R. Leitgeb, C. K. Hitzenberger, and A. F. Fercher, "Performance of fourier domain vs. time domain optical coherence tomography," *Opt. Express* 11, 889–894 (2003).

요 약 문

바이매뉴얼 미세수술을 위한

듀얼 스마트 시스템에 대한 연구

매뉴얼 방식의 정밀 수술 기법은 기본적으로 잡고, 자르고 주입하는 조작이 생물학적 시편에서 시행된다. 망막 표면으로부터의 효율적인 파이브로스 시편의 절단은 주로 잡고 자르는 조작을 동시적으로 수행하는 것을 필요로 한다. 실제 바이매뉴얼 수술은 의사가 양손의 타고난 손 떨림과 예측할 수 없는 환자의 움직임을 요구한다.

본 연구에서 우리는 듀얼 스마트 시스템을 개발하고 평가했다. 듀얼 스마트 시스템은 볼렌즈와 결합된 두 개의 공통 경로 파장가변 광결맞음 단층 촬영 거리 센서 (CP SS-OCT), 두 개의 피에조 모터와 개조된 수평 가위와 포셉으로 구성된다. 볼렌즈와 결합된 OCT 거리 센서는 45 도에서 90 도 사이의 기울기에서 양손의 예기치 못한 손 떨림을 측정할 수 있다. 또한, 높은 개구수(NA)가진 볼렌즈가 결합된 OCT 거리센서는 기존 OCT 거리 센서보다 1.3 배 높은 신호 대 잡음 비를 가진다.

듀얼 스마트 시스템은 효율적인 바이매뉴얼 절단을 위해서 수술 도구 말단자 각각의 설정 높이를 조작할 수 있다. 시스템의 전체 피드백 속도는 500 Hz 로 6-12Hz 의 손 떨림을 보상하기 충분히 빠르다. 추가적으로, 기존 가위와 포셉을 개조함으로써 기존 수직 가위와 포셉보다 수술 영역의 접근성 향상에 기여할 수 있었다.

볼렌즈가 결합된 듀얼 스마트 시스템은 물에서도 예기치 않은 손 떨림을 다양한 각도에서 보상할 수 있었다. 이 시스템은 맨손보다 정밀하게 난간 막 절단할 수 있었을 뿐만 아니라 RMSE 또한 맨손보다 10 배가량 낮았다. 더욱이 시스템에 의해 절단된 면은 매우 균일했다. 높은 SNR 을 가진 시스템은 돼지 눈 실험에서도 맨손보다 월등히 나은 손 떨림 보상을 능력을 증명했다.

이 시스템을 사용함으로써 바이매뉴얼 유리체 망막 수술 중 발생할 수 있는 의사 부주의로 인한 손상을 최소화 할 수 있다. 향후, 안정적인 미세 수술이 가능하도록 듀얼 스마트 시스템의 내구성을 향상 시킬 것이다.

핵심어: 광 단층 촬영 장치, 바이매뉴얼 수술, PZT 모터, 볼렌즈, 듀얼 스마트 시스템, 수평 가위, 수평 폴셉